doi:10.1016/j.jmb.2008.04.006 J. Mol. Biol. (2008) 379, 568–578

JMB

Available online at www.sciencedirect.com

ScienceDirect

ELSEVIER

Molecular Mechanism of ADP-Ribose Hydrolysis By Human NUDT5 From Structural and Kinetic Studies

Manwu Zha[1]†, Qing Guo[1]†, Yichun Zhang[2], Biao Yu[2], Ying Ou[1], Chen Zhong[1]* and Jianping Ding[1]*

[1]*State Key Laboratory of Molecular Biology, Institute of Biochemistry and Cell Biology, Shanghai Institutes for Biological Sciences, Chinese Academy of Sciences, 320 Yue-Yang Road, Shanghai 200031, China*

[2]*State Key Laboratory of Bio-organic and Natural Products Chemistry, Shanghai Institute of Organic Chemistry, Chinese Academy of Sciences, 354 Feng-Ling Road, Shanghai 200032, China*

Received 28 January 2008; received in revised form 31 March 2008; accepted 2 April 2008
Available online
8 April 2008

Human NUDT5 (hNUDT5) is an ADP-ribose (ADPR) pyrophosphatase (ADPRase) that plays important roles in controlling the intracellular levels of ADPR and preventing non-enzymatic ADP-ribosylation of proteins by hydrolyzing ADPR to AMP and ribose 5′-phosphate. We report the crystal structure of hNUDT5 in complex with a non-hydrolyzable ADPR analogue, α,β-methyleneadenosine diphosphoribose, and three Mg^{2+} ions representing the transition state of the enzyme during catalysis. Analysis of this structure and comparison with previously reported hNUDT5 structures identify key residues involved in substrate binding and catalysis. In the transition-state structure, three metal ions are bound at the active site and are coordinated by surrounding residues and water molecules. A conserved water molecule is at an ideal position for nucleophilic attack on the α-phosphate of ADPR. The side chain of Glu166 on loop L9 changes its conformation to interact with the conserved water molecule compared with that in the substrate-bound structure and appears to function as a catalytic base. Mutagenesis and kinetic studies show that Trp28 and Trp46 are important for the substrate binding; Arg51 is involved in both the substrate binding and the catalysis; and Glu112 and Glu116 of the Nudix motif, Glu166 on loop L9, and Arg111 are critical for the catalysis. The structural and biochemical data together reveal the molecular basis of the catalytic mechanism of ADPR hydrolysis by hNUDT5. Specifically, Glu166 functions as a catalytic base to deprotonate a conserved water molecule that acts as a nucleophile to attack the α-phosphate of ADPR, and three Mg^{2+} ions are involved in the activation of the nucleophile and the binding of the substrate. Structural comparison of different ADPRases also suggests that most dimeric ADPRases may share a similar catalytic mechanism of ADPR hydrolysis.

Keywords: Nudix domain; ADPR; ADP-ribose pyrophosphatase; NUDT5; molecular mechanism

Edited by M. Guss

Introduction

Nudix pyrophosphatases are a family of enzymes that catalyze the hydrolysis of *nu*cleoside *di*phosphates linked to another moiety *X* in the presence of Mg^{2+} or other divalent cations. These enzymes share a highly conserved Nudix motif ($GX_5EX_7REUXEEXGU$, where U is usually one of the bulky hydrophobic amino acids I, L, and V) that forms a loop–helix–loop structure and is involved in the binding of the metal ions.[1,2] Substrates of the Nudix enzymes include 8-oxo-deoxy-GTP, dinucleoside polyphosphates, and other metabolic intermediates that are potentially harmful to cells when they accumulate.[1,3] ADP-ribose (ADPR) is one of these substrates that is generated by turnover of NAD^+, cyclic ADPR, and protein-bound poly- and mono-ADPR.[4] ADP-ribosylation of proteins, like phosphorylation, is a post-translational modification that can modulate protein

*Corresponding authors. E-mail addresses: czhong@sibs.ac.cn; jpding@sibs.ac.cn.

† M.Z. and Q.G. contributed equally to this work.

Abbreviations used: hNUDT5, human NUDT5; ADPR, ADP-ribose; ADPRase, ADP-ribose pyrophosphatase; EcADPRase, *Escherichia coli* ADPRase; MtADPRase, *Mycobacterium tuberculosis* ADPRase; TtADPRase, *Thermus thermophilus* ADPRase; R5P, ribose 5′-phosphate; AMPCPR, α,β-methyleneadenosine diphosphoribose.

functions. A growing body of evidence has shown that ADP-ribosylation of proteins is critical in various important cellular processes, such as regulation of mitosis, regulation of telomere length and longevity, gene transcription, cellular proliferation and differentiation, and cell death, and thus may influence physiological and pathophysiological outcomes, including carcinogenesis, inflammation, and neuronal functions (reviewed in the work of Haag and Koch-Nolte[5] and Hassa *et al.*[6]). The damage caused by undesired ADP-ribosylation of proteins has been well demonstrated by bacterial toxins, such as diphtheria, cholera, and pertussis toxins, which are bacterial mono-ADP-ribosyl transferases and would interfere with the fundamental processes of host cells, such as signal transduction mechanisms and protein synthesis, and ultimately cause cell death (reviewed in the work of Ueda and Hayaishi[7] and McDonald and Moss[8]). High concentrations of intracellular ADPR could lead to non-enzymatic ADP-ribosylation of proteins by modifying histidinyl, lysyl, and cysteinyl residues and might interfere with normal cellular functions, a process that is suggested to be deleterious.[9,10] Moreover, free ADPR might function as a second messenger to regulate calcium signaling.[11,12] Therefore, the intracellular levels of free ADPR should be tightly controlled.

ADPR pyrophosphatases (ADPRases) are the enzymes responsible for controlling cellular ADPR levels by hydrolyzing ADPR to AMP and ribose 5′-phosphate (R5P), which can be further recycled by several metabolic pathways.[4] The activities of ADPRases have been found in all three kingdoms of life. These enzymes exhibit great divergence in substrate specificity and metal ion selectivity and probably also differ in their catalytic mechanism.[13] Structural studies of *Escherichia coli* ADPRase (EcADPRase) reveal an associative mechanism in which a conserved water molecule is activated by two of the three metal ions at the active site and poised for nucleophilic attack on the α-phosphate of the substrate; that Glu112 and Glu116 of the Nudix motif are involved in the coordination of the metal ions; and that Glu162, which is located on a loop close to the Nudix motif, acts as the catalytic base to deprotonate the water molecule.[2,13,14] Mutation of residue Glu142, equivalent to Glu162 of EcADPRase, in *Mycobacterium tuberculosis* ADPRase (MtADPRase) causes an approximately 320-fold decrease in k_{cat} and an approximately 3.2-fold increase in K_m, suggesting that MtADPRase might share a similar catalytic mechanism with EcADPRase.[13,15] However, a different catalytic mechanism was proposed for *Thermus thermophilus* ADPRase (TtADPRase) Ndx4 because only two metal ions are found to bind at the active site and thus are suggested to be involved in activation of a conserved water molecule that acts as the nucleophile to attack the α-phosphate of the substrate, and mutation of Glu127, which is considered to be equivalent to Glu162 of EcADPRase, has no effect on the enzymatic activity.[16–18] Intriguingly, in the structure of another TtADPRase Ndx2, there are three metal ions bound at the active site and mutation of Glu136 (corresponding to Glu162 of EcADPRase) does decrease k_{cat} by about 12-fold.[18]

For eukaryotes, crystal structures of two human ADPRases (hNUDT9 and hNUDT5) have been reported.[19,20] The two enzymes belong to different groups and show distinct characteristics: hNUDT9 is active as a monomer and is highly specific for ADPR,[19,21] whereas hNUDT5 exists as a homodimer and can utilize a variety of ADP–sugar conjugates as the substrate, with a preference for ADPR.[20,22,23] The catalytic mechanisms of both enzymes remain yet unclear. As the complex of hNUDT9 with ADPR has not been obtained, a model of the complex was built based on the crystal structures of hNUDT9 in apo form and in complex with the product R5P. Mutagenesis studies show that the residue structurally equivalent to Glu162 of EcADPRase does not appear to be critical for the catalytic reaction.[19] For hNUDT5, analyses of the crystal structures of hNUDT5 in apo form and in complex with substrate ADPR or product AMP in our previous study indicated that hNUDT5 has a structure similar to that of EcADPRase and functions as a homodimer; in addition, in the structure of the hNUDT5–AMP–Mg^{2+} complex, three metal ions are bound at the active site to mediate the interactions between the α-phosphate of AMP and the enzyme.[20] Here we report the crystal structure of hNUDT5 in complex with a non-hydrolyzable ADPR analogue, α,β-methyleneadenosine diphosphoribose (AMPCPR), and three Mg^{2+} ions representing the transition state of the enzyme during catalysis. Structural analysis of this complex and comparison with other hNUDT5 structures identify key residues that play important roles in the recognition and binding of the substrate and the catalytic reaction. The functional roles of these residues are further confirmed by mutagenesis and kinetic studies. The structural and biochemical data together reveal the molecular basis for the catalytic mechanism of hNUDT5.

Results and Discussion

Structure of hNUDT5 in complex with AMPCPR and Mg^{2+}

To understand the catalytic mechanism of ADPR hydrolysis by hNUDT5, we determined the crystal structure of a truncated hNUDT5 (residues 1–210, ΔhNUDT5) in complex with a substrate analogue, AMPCPR, and Mg^{2+} ions that represent the transition state of the catalytic reaction. The complex structure has been refined to 2.0-Å resolution with an *R*-factor of 0.198 and a free *R*-factor of 0.233. A summary of the structure refinement and the final model statistics is given in Table 1. We previously showed that deletion of the nine C-terminal residues of hNUDT5 (residues 1–210, ΔhNUDT5) can facilitate formation of crystals of the enzyme in complex with ADPR or AMP with high diffraction quality; ΔhNUDT5 has enzymatic activity in crystals and

Table 1. Statistics of diffraction data and structure refinement

Statistics of diffraction data	
Space group	*C*2
Unit cell parameters	
a/*b*/*c* (Å)	113.4/41.2/99.6
β (°)	121.7
Wavelength (Å)	1.0000
Resolution (Å)[a]	50.0–2.00 (2.07–2.00)
Observed reflections	139,306
Unique reflections	26,406
Mosaicity	0.57
Redundancy	5.3 (5.2)
$I/\sigma(I)$	25.3 (15.5)
Completeness (%)	98.4 (98.8)
R_{merge} (%)[b]	4.8 (9.3)
Statistics of refinement and structural model	
R_{cryst}[c]/R_{free}[d] (%)	19.8/23.3
No. of amino acids (atoms)	410 (3032)
No. of water molecules	242
No. of metal ions	6
No. of ligands	2
Average *B*-factor of protein atoms (Å^2)	31.1
Average *B*-factor of metal ions (Å^2)	37.7
Average *B*-factor of ligands (Å^2)	41.3
RMSD bond lengths (Å)	0.005
RMSD bond angles (°)	0.82
Luzzati atomic positional error (Å)	0.22
Ramachandran plot (%)	
Most favored	90.3
Allowed	9.7

[a] The numbers in parentheses refer to the highest-resolution shell.
[b] $R_{merge} = \Sigma_{hkl}\Sigma_i \mid I_i(hkl)_i - \langle I(hkl)\rangle \mid / \Sigma_{hkl}\Sigma_i(hkl)$.
[c] $R_{cryst} = \Sigma \mid\mid F_o \mid - \mid F_c \mid\mid / \Sigma \mid F_o \mid$.
[d] R_{free} is monitored with 5% of randomly selected reflections.

assumes an overall structure similar to that of the full-length enzyme; and the omitted C-terminal residues do not participate in substrate binding or dimerization.[20] Here we further show that ΔhNUDT5 has comparable enzymatic activity and kinetic characteristics similar to those of the full-length enzyme (Table 2). Therefore, ΔhNUDT5 will not be distinguished from the full-length hNUDT5 unless otherwise specified in the following discussion.

In the AMPCPR-bound complex, the enzyme forms a homodimer in the asymmetric unit, with each subunit consisting of an N-terminal domain (residues 1–96) and a C-terminal Nudix domain (residues 97–210) (Fig. 1a). The dimer displays substantial domain swapping such that the N-terminal domain of one subunit crosses over to interact with the C-terminal domain of the other to form a major portion of the dimer interface, a characteristic feature of the dimeric ADPRases. The active site is located at the dimer interface and mainly consists of structural elements L3, L5, L8*, L9, and the Nudix motif (loop L6–helix α1–loop L7) of the Nudix domain and L1 and β3* of the N-terminal domain (the nomenclature of the secondary structures of hNUDT5 is after that of Zha *et al.*,[20] and the structural elements and residues from the adjacent subunit are indicated with an asterisk hereafter) (Fig. 1b). There are one AMPCPR molecule and three Mg^{2+} ions bound at each active site with well-defined electron density.

The bound AMPCPR has extensive hydrogen-bonding and hydrophobic interactions with the surrounding residues (Fig. 1c). The adenine N1 and N6 atoms are recognized via hydrogen-bonding interactions by the main-chain amide (3.1 Å) and carbonyl (3.1 Å), respectively, of the conserved Glu47*. The adenine N7 forms hydrogen bonds with the side-chain Nη1 of Arg51 (3.1 Å) directly and Nη2 indirectly via a conserved water molecule (Wat1). The adenine moiety is sandwiched between the side chains of Trp28 and Trp46* via π–π stacking interactions. These interactions are the same as those observed in the hNUDT5–ADPR complex.[20] The negative charges on the pyrophosphate group of AMPCPR are partially neutralized by a conserved residue Arg84 via two hydrogen bonds (2.2 and 2.5 Å, respectively). The terminal ribose is pointing toward the L8* loop, with both hydroxyl groups forming hydrogen bonds with the side chain of Asp133* (2.2 and 2.5 Å, respectively).

There are three Mg^{2+} ions bound at the active site (Fig. 1c). Two Mg^{2+} ions (M1 and M2) are situated between the α-phosphate of AMPCPR and the Nudix motif. M1 has five coordination ligands, including one α-phosphate oxygen (2.5 Å), one carboxylate oxygen of Glu112 (2.6 Å), and three water molecules (2.5–2.8 Å) in a square pyramidal geometry. M2 is coordinated by one α-phosphate oxygen (2.7 Å), one carboxylate oxygen each of Glu112 (2.5 Å) and Glu116 (2.5 Å), and three water molecules (2.5–2.9 Å) in an octahedral geometry. M3 is located between the α- and β-phosphates of AMPCPR and is coordinated by one α-phosphate oxygen (2.5 Å), one β-phosphate oxygen (2.1 Å), one carboxylate oxygen of Glu116 (2.2 Å), the main-chain carbonyl oxygen of Ala96 (2.3 Å), and two water molecules (2.2–2.3 Å) in an octahedral geometry as well. A conserved water molecule (Wat2) bridges M1 and M2 and is almost perfectly in line with the "scissile" bond (the angle of water–phosphorus–methylene carbon is about 175°), which appears to function as the nucleophile (see discussion later).

Structural comparisons of the hNUDT5–AMPCPR–Mg^{2+} complex (transition state) with the hNUDT5–ADPR–Mg^{2+} complex (pre-transition state) and the hNUDT5–AMP–Mg^{2+} complex (product state) show that the overall structures are very similar (RMSD values of about 0.57 and 0.62 Å, respectively, for 412 C^{α} atoms) (Fig. 1d and e). The substrate analogue AMPCPR binds at the substrate-binding pocket in a position similar to that of ADPR and AMP. However, notable differences are observed at the active site among the three complexes. In the AMPCPR-bound complex, three Mg^{2+} ions are present, and one of them (M3) occupies a similar position as the only Mg^{2+} ion observed in the ADPR-bound complex. Although the main chains of the surrounding residues remain the same, the side-chain orientations of residues Glu112 and Glu166 are changed to coordinate with the metal ions (Fig. 1d). As a result, loop L9 (residues 156–167) and the Nudix motif (residues 102–117) composing the active site are more stabilized, which is also manifested by their significantly

Table 2. Kinetic data for ADPR hydrolysis by wild-type and mutant hNUDT5

	K_m (μM)	Change in K_m	k_{cat} (s^{-1})	Change in k_{cat}	k_{cat}/K_m (M^{-1} s^{-1})
Wild type[a]	20.4±0.1		11.4±0.1		5.6×10^5
Wild type	22.3±2.2		11.8±0.1		5.3×10^5
ΔhNUDT5	21.4±1.9		12.7±0.1		5.9×10^5
Recognition of the adenosine moiety					
W28A	184.0±11.5	↑8.4-fold	13.3±0.4		7.2×10^4
W46A	126.5±10.3	↑5.7-fold	11.3±0.2		8.9×10^4
W28A–W46A	149.7±125.9	↑53.7-fold	$(5.8\pm0.3)\times10^{-2}$	↓219-fold	5.0×10^1
R51Q	321.3±21.1	↑14.6-fold	$(4.1\pm0.1)\times10^{-1}$	↓17-fold	1.2×10^3
Recognition of the phosphates and the terminal ribose moiety					
Q82A	127.1±6.1	↑5.8-fold	10.3±0.1		8.1×10^4
R84Q	108.4±15.9	↑4.9-fold	$(1.8\pm0.1)\times10^{-1}$	↓67-fold	1.7×10^3
E93Q	38.9±2.9	↑1.8-fold	4.5±1.0		1.2×10^5
L98A	128.3±5.0	↑5.8-fold	12.4±0.6		9.7×10^4
D133N	45.6±6.1	↑2.1-fold	10.4±0.6		2.3×10^5
D133A	87.9±7.7	↑4.0-fold	7.3±0.2		8.3×10^4
C139A	46.3±3.7	↑2.1-fold	13.7±0.4		3.0×10^5
R196Q	119.7±13.4	↑5.5-fold	6.0±0.1		5.0×10^4
Catalysis					
R111Q	27.9±1.9		$(3.2\pm0.2)\times10^{-1}$	↓34-fold	1.3×10^4
E112Q	70.2±7.3	↑3.2-fold	$(1.9\pm0.3)\times10^{-3}$	↓6300-fold	2.7×10^1
E115Q	40.2±4.3	↑1.8-fold	2.7±0.1	↓4-fold	6.7×10^4
E116Q	25.7±4.1		$(6.9\pm0.5)\times10^{-3}$	↓2000-fold	2.3×10^2
D164A	43.4±2.5	↑1.4-fold	12.2±0.9		3.9×10^5
D164N	20.9±0.9		13.1±0.8		6.3×10^5
E166Q	23.1±1.6		$(1.0\pm0.1)\times10^{-1}$	↓120-fold	4.3×10^3

[a] These data were measured with the method described by Yoshiba *et al.*[16] for comparison with the data obtained with the new method.

lowered *B*-factors (55.8 *versus* 77.1 $Å^2$ for the L9 loop and 28.0 *versus* 38.4 $Å^2$ for the Nudix motif, respectively) with better defined electron density, albeit the average *B*-factors of the two complexes are comparable (31.7 *versus* 37.5 $Å^2$). In particular, the *B*-factors of residues Glu112, Glu116, and Glu166 that are directly or indirectly involved in metal binding decrease substantially from 43.4, 48.8, and 89.3 $Å^2$ to 25.5, 24.4, and 54.7 $Å^2$, respectively.

In the AMP-bound complex, the product AMP has a notable movement after hydrolysis of ADPR and release of R5P and, particularly, the α-phosphate group moves closer to the Nudix motif by about 0.7 Å compared with the AMPCPR-bound complex (Fig. 1e). Correspondingly, two of the three Mg^{2+} ions (M1 and M2) move toward the Nudix motif as well, whereas the position of M3 remains unchanged. These metal ions have incomplete coordination geometry and relatively higher *B*-factors. Moreover, the conserved water molecule observed in the hNUDT5–AMPCPR–Mg^{2+} complex is absent. Therefore, the side chain of Glu166 assumes a similar position as in the ADPR-bound complex and coordinates with M2. The side chain of Glu112 of the Nudix motif also rotates slightly to have coordination with both M1 and M2.

Kinetic studies of the wild-type and mutant hNUDT5

Based on structural analyses of the hNUDT5–AMPCPR–Mg^{2+} complex and the previously reported hNUDT5 complexes with ADPR and AMP,[20] we are able to identify the key residues that might be involved in the recognition and binding of the substrate and/or the catalytic reaction. To validate the functional roles of these residues, we performed mutagenesis and kinetic studies. The enzymatic activities of both wild-type and mutant hNUDT5 were assayed using a more rapid and sensitive method developed based on two methods described previously.[16,24]

First, we examined the residues involved in the recognition and binding of the adenosine moiety of the substrate. In all structures of hNUDT5 in complex with ADPR, AMPCPR, or AMP, residues Trp28 and Trp46* sandwich the adenine moiety via π–π stacking interactions; thus, substitution of these two residues with Ala would abolish the interactions and weaken substrate binding. In addition, one side-chain amide group of Arg51 forms a hydrogen bond with the adenine N7, and the other interacts with one hydroxyl group of the adenosyl ribose moiety; thus, this residue appears to be essential in maintaining the horseshoe-shaped conformation of the substrate. Indeed, single-mutation W28A or W46A causes a reduced binding affinity for ADPR, with the K_m value increased by 8.4-fold for the former and 5.7-fold for the latter, but has no significant effect on the k_{cat} value. However, the double-mutation W28A–W46A confers a markedly increased K_m (53.7-fold) and a substantially decreased k_{cat} (219-fold), indicating that Trp28 and Trp46* function synergistically in substrate binding and catalysis (Table 2). Similarly,

mutation R51Q causes a marked increase of K_m (14.6-fold) and a decrease of k_{cat} (17-fold), confirming the critical role of this residue in both substrate binding and catalysis (Table 2).

Next, we tested the residues involved in the recognition and binding of the phosphates and the terminal ribose moiety of the substrate. The structures of hNUDT5 show that Leu98 is located near the

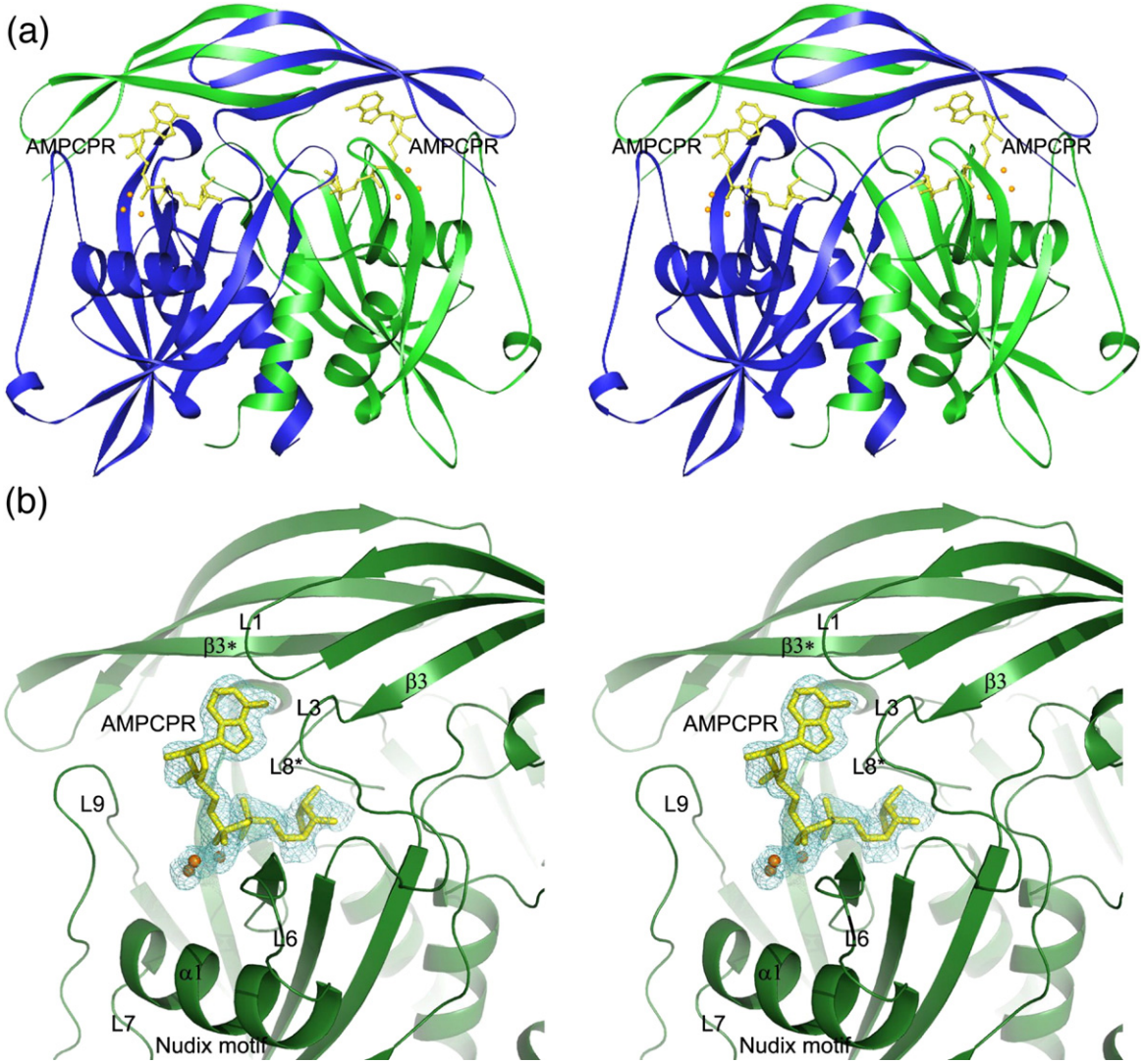

Fig. 1. Structure of the hNUDT5–AMPCPR–Mg^{2+} complex. (a) Stereoview of the overall structure. The enzyme forms a homodimer (one subunit shown in green; the other, in blue), and the active site is composed of structural elements of the N-terminal domain of one subunit and the Nudix domain of the other. The bound AMPCPR molecules are shown with yellow ball-and-stick models, and the metal ions are shown with golden spheres. (b) Stereoview of the structure of the catalytic active site. The secondary structural elements composing the active site are labeled. The $F_o - F_c$ electron density map (contour level, 2σ) for the bound AMPCPR and metal ions is shown with cyan meshes. (c) Stereoview of the interactions between AMPCPR and the surrounding residues. The three Mg^{2+} ions are shown as golden spheres, and the conserved water molecules are shown as red spheres; also shown are surrounding residues with side chains, with those from the first subunit in gray and those from the second subunit in cyan and indicated with an asterisk. Carbon is shown in yellow; oxygen, red; nitrogen, blue; and phosphorus, magenta. The hydrogen-bonding interactions are indicated with broken lines. (d) Comparison of the active site between the hNUDT5–AMPCPR–Mg^{2+} (in green) and hNUDT5–ADPR–Mg^{2+} (in gray) complexes. Three key residues (Glu112, Glu116, and Glu166) are shown with side chains. AMPCPR and ADPR are shown with yellow and gray ball-and-stick models, respectively. Three Mg^{2+} ions (golden spheres) and a conserved water molecule (red sphere) are present in the hNUDT5–AMPCPR–Mg^{2+} complex, whereas only one Mg^{2+} ion (gray sphere) is observed in the hNUDT5–ADPR–Mg^{2+} complex. Despite the similarity of the overall structures of the two complexes, the side chains of residues Glu112 and Glu166 have substantially different conformations. (e) Comparison of the active site between the hNUDT5–AMPCPR–Mg^{2+} (in green) and hNUDT5–AMP–Mg^{2+} (in gray) complexes. Residues Glu112, Glu116, and Glu166 are shown with side chains. AMPCPR and AMP are shown with yellow and gray ball-and-stick models, respectively. There are three Mg^{2+} ions bound at the active site in both hNUDT5–AMPCPR–Mg^{2+} (golden spheres) and hNUDT5–AMP–Mg^{2+} (gray spheres) complexes. Due to the subtle positional differences of the metal ions and the absence of the conserved water molecule, the side chains of residues Glu112 and Glu166 in the product state assume different conformations compared with those in the transition state.

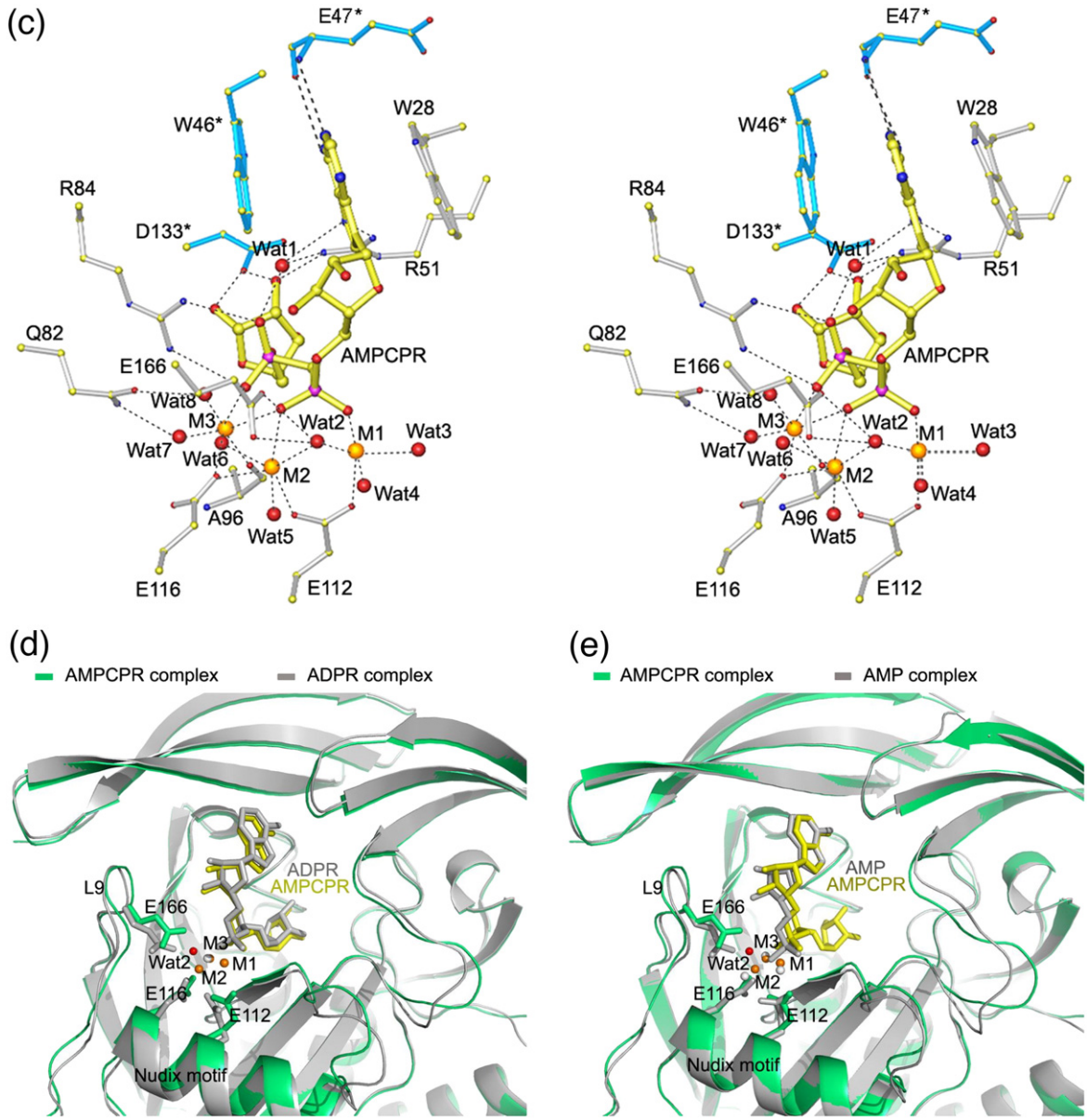

Fig. 1 (*legend on previous page*)

two phosphates (3–4 Å). The kinetic data show that mutation of Leu98 to Ala causes a 5.8-fold increase in K_m but has no effect on k_{cat}, indicating that this residue is primarily involved in substrate binding (Table 2). The side-chain amino groups of the conserved Arg84 neutralize the negative charges of the β-phosphate via two hydrogen-bonding interactions. Removal of the positively charged group by mutating Arg84 to Gln abrogates these interactions and leads to a 4.9-fold increase in K_m and a 67-fold decrease in k_{cat}, indicating that Arg84 is involved in both substrate binding and catalysis. In addition, the side chain of Gln82 has hydrogen-bonding interactions with two water molecules (Wat6 and Wat7) that are involved in coordination of metal ion M3. Mutation of Gln82 to Ala causes a 5.8-fold increase in K_m but has no effect on k_{cat}, suggesting that Gln82 is probably involved in substrate binding via the metal ion. In the structure of the AMPCPR-bound hNUDT5 complex, the recognition of the terminal ribose moiety is mainly mediated by the side chain of Asp133∗ via two hydrogen-bonding interactions with the two hydroxyl groups. In addition, the side chains of Glu93, Cys139, and Arg196 interact indirectly with the free hydroxyl group of the terminal ribose via several water molecules. Similar interactions are also observed in the ADPR-bound hNUDT5 complex.[20] Kinetic data show that mutations of these residues have minor effects on K_m (4.0-, 2.1-, 1.8-, 2.1-, and 5.5-fold increases for D133A∗, D133N∗, E93Q, C139A, and R196Q, respectively) but no effect on k_{cat}, indicating that the binding of the terminal ribose

moiety plays a less critical role in substrate binding and catalysis.

Residues that are probably involved in catalysis were also investigated. As it has been shown that the metal ions play an important role in the catalytic reaction for ADPRases,[15,16,22,25] the residues that have direct and indirect interactions with the metal ions in the structures of hNUDT5 were selected for mutagenesis studies (Table 2). In the structures of hNUDT5, residues Arg111, Glu112, Glu115, and Glu116 of the Nudix motif all point their side chains toward the active site, and, in particular, Glu112 and Glu116 are directly involved in coordination of the metal ions. Consistently, kinetic data show that both mutations E112Q and E116Q cause dramatic decrease in k_{cat} (6.3×10^3 and 2.0×10^3, respectively), albeit their effects on K_m are minor, indicating that these two residues are critical for the binding of the metal ions and the catalytic reaction. On the other hand, mutations R111Q and E115Q have less significant effects on k_{cat} (decreased by 34- and 4-fold, respectively) and minor effects on K_m, in agreement with their indirect involvement in metal binding and catalysis.

In the crystal structure of the EcADPRase–AMPCPR–Mg^{2+} complex, Glu162-containing loop L9 moves from its position in the apo enzyme toward the active site by about 10 Å and makes a sharp turn to bring Glu162 to a proper position to interact with a conserved water molecule; thus, it was proposed that Glu162 functions as a catalytic base to deprotonate the conserved water that further carries out the hydrophilic attack on the α-phosphate of ADPR in hydrolysis.[14] Sequence and structural alignments of the ADPR-bound hNUDT5 and EcADPRase complexes show that hNUDT5 contains an Asp residue (Asp164) at the equivalent position.[20] However, in the structure of the hNUDT5–AMPCPR–Mg^{2+} complex, Asp164 points its side chain outward and does not appear to be involved in the catalytic reaction. To examine its functional role, we mutated Asp164 into either Gln or Ala and performed the kinetic studies of these mutants (Table 2). The very little effects on both K_m and k_{cat} by these mutations suggest that Asp164 is not involved in substrate binding or catalysis and therefore cannot be a general base. Interestingly, Glu166, another residue on loop L9, interacts indirectly with metal ion M2 via a conserved water molecule in the AMPCPR-bound complex (Fig. 1c). Furthermore, mutation E166Q results in a 120-fold decrease of k_{cat} but has no effect on K_m, indicating that Glu166 plays an important role in the catalytic reaction.

Catalytic mechanism of hNUDT5

When the hNUDT5–AMPCPR–Mg^{2+} complex is compared with the hNUDT5–ADPR–Mg^{2+} complex, loop L9 does not move; however, the side chain of Glu166 rotates toward the active site upon the binding of additional two metal ions and forms hydrogen bonds with a conserved water molecule (Wat2) that coordinates with both metal ions M1 and M2 (Fig. 1d). This water molecule is positioned about 4.2 Å away from the α-phosphorus and is in line with the adenosyl-phosphorus and the methylene carbon of the substrate (the angle is about 175°). Therefore, it is at an ideal position to carry out the nucleophilic attack on the α-phosphate of ADPR.

Based on the structural and biochemical data, we propose here a model for the catalytic mechanism of ADPR hydrolysis by hNUDT5 (Fig. 2a). Specifically, upon binding of the three metal ions, the catalytic base Glu166 reorients its side chain toward the active site to abstract a proton from the nucleophilic water molecule that is rendered more reactive by virtue of binding to metal ions M1 and M2. The resultant hydroxide carries out the nucleophilic attack on the α-phosphate of ADPR, leading to the hydrolysis of ADPR into AMP and R5P. As described previously, supplementation of extra Mg^{2+} to the crystal of the hNUDT5–ADPR–Mg^{2+} complex resulted in hydrolysis of the substrate and yielded the hNUDT5–AMP–Mg^{2+} complex with three Mg^{2+} ions bound at the active site.[22] Therefore, it is likely that after hydrolysis, R5P might leave, with the negative charge of the phosphate being neutralized by Arg84, and AMP might remain bound at the active site, with the negative charges of the phosphate being neutralized by the metal ions until being replaced by ADPR.

Comparison of the catalytic mechanisms of ADPR hydrolysis by different ADPRases

Previously, the catalytic mechanisms of ADPR hydrolysis by several dimeric bacterial ADPRases have been proposed.[14,15,17,18] It has been shown that for EcADPRase, loop L9 undergoes significant conformational changes during catalysis and Glu162 on loop L9 acts as the general base to deprotonate a water molecule that further functions as the attacking nucleophile.[14] As the structural comparison of the hNUDT5–AMPCPR–Mg^{2+} complex and the EcADPRase–AMPCPR–Mg^{2+} complex shows that Asp164 of hNUTD5 occupies a similar position as that of Glu162 of EcADPRase, Asp164 was thought to be the equivalent residue to function as a general base. However, neither the conformation nor the position of Asp164 is changed during the catalysis and mutagenesis of this residue results in little change of the enzymatic activity. Instead, Glu166 is implicated to function as the catalytic base. Therefore, although our proposed catalytic mechanism of ADPR hydrolysis by hNUDT5 is in principle similar to that by EcADPRase, there are notable differences between the two models. Specifically, loop L9 of hNUDT5 does not change conformation during catalysis and the proposed general base Glu166 occupies a different position on loop L9 in the AMPCPR-bound complex (Fig. 2b). Moreover, the loops surrounding the active site, especially loop L9, are quite different (Fig. 2b). In particular, Glu166 of hNUDT5 occupies a position after the L9 turn, whereas Glu162 of EcADPRase is located at the tip of the L9 turn, which is about two residues ahead of the equivalent posi-

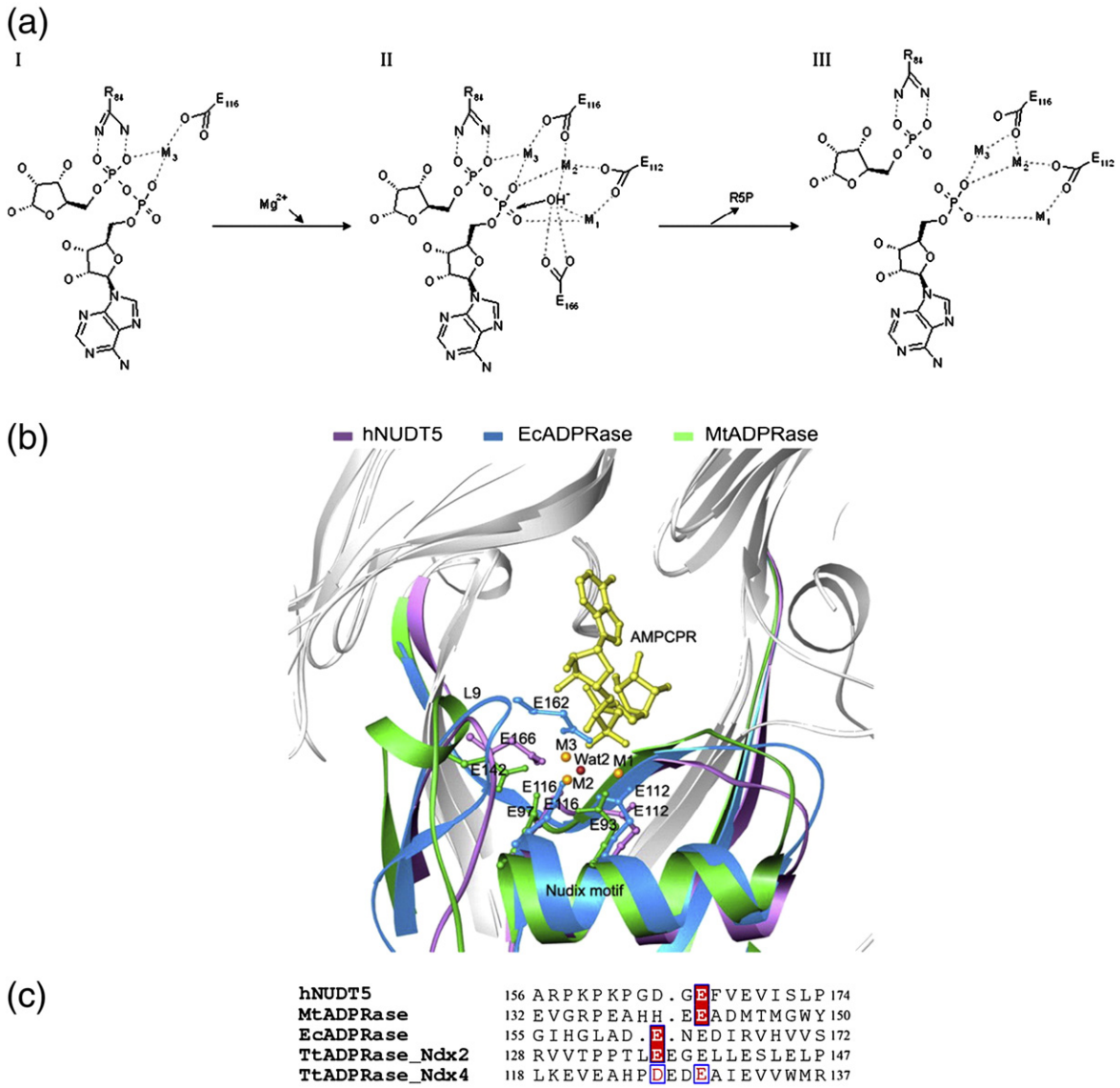

Fig. 2. Catalytic mechanism of ADPR hydrolysis by hNUDT5. (a) Schematic presentation of the catalytic mechanism of ADPR hydrolysis by hNUDT5. I, ADPR-bound pre-transition state. II, AMPCPR-bound transition state. III, AMP-bound product state. A conserved water molecule bridges the metal ions M1 and M2 and acts as the nucleophile to attack on the adenosyl phosphorus after being deprotonated by the catalytic base Glu166. (b) Comparison of the active site among the structures of hNUDT5 (in magenta), EcADPRase (in blue), and MtADPRase (in green) in their respective complexes with AMPCPR and metal ions. For clarity, only AMPCPR (yellow ball-and-stick model), the three metal ions (golden spheres), and the conserved water molecule (red sphere) in the structure of the hNUDT5–AMPCPR–Mg^{2+} complex are shown. The key residues Glu112, Glu116, and Glu166 of hNUDT5 that are involved in metal binding are shown with side chains in magenta, and those of EcADPRase (Glu112, Glu116, and Glu162) and MtADPRase (Glu93, Glu97, and Glu142) are shown in blue and green, respectively. (c) Structure-based sequence alignment of the loops containing the catalytic base in different ADPRases. The residues of hNUDT5, MtADPRase, EcADPRase, and TtADPRase Ndx2 are structurally aligned based on their positions in the respective structures of the AMPCPR-bound complexes. Because TtADPRase Ndx4 has no structure of the AMPCPR-bound complex, the residues of Ndx4 are aligned with those of Ndx2 based on sequence similarity between the two enzymes. Glu166 of hNUDT5, Glu142 of MtADPRase, Glu162 of EcADPRase, and Glu136 of Ndx2 are proposed to function as the catalytic base based on structural and kinetic data and are denoted with filled red boxes. Asp126 and Glu129 of Ndx4 (denoted with open red box) may play a similar role, but their functions need to be further determined.

tion of Glu166 (Fig. 2b and c). In MtADPRase,[15] the general base Glu142 is situated at the same position as Glu166 of hNUDT5 rather than Glu162 of EcADPRase. Also, the biochemical data have shown that mutation E166Q in hNUDT5 and mutation E142Q in MtADPRase[13] result in comparable decreases in k_{cat} (about 120- and 320-fold, respectively). Loop L9 of MtADPRase is only stabilized when the substrate and three metal ions are bound at the active site, suggesting that conformational change of loop L9 may take place during catalysis. Regardless of the differences in the conformation and/or movement of loop

L9 and the respective positions of the proposed catalytic bases, hNUDT5, MtADPRase, and EcADPRase share a similar catalytic mechanism as these catalytic bases are structurally close to and form hydrogen bonds with the conserved water molecule that acts as the nucleophile in the complex structure with AMPCPR and metal ions and assume the same function in catalysis.

On the other hand, the dimeric thermophilic bacterial TtADPRase Ndx4 has been suggested to utilize a different mechanism because Glu127, which was thought to be equivalent to Glu162 of EcADPRase, is not essential for catalysis and only two metals ions that occupy the positions approximately equivalent to those of M2 and M3 in the hNUDT5–AMPCPR–Mg^{2+} complex are observed to bind at the active site in the structure of the Ndx4–ADPR–Gd^{3+} complex.[16] Thus, a two-metal-ion mechanism was proposed for TtADPRase Ndx4 in which a water molecule is activated to act as the nucleophile by two divalent cations that are coordinated by Glu82 and Glu86 (equivalent to Glu112 and Glu116 of hNUDT5, respectively).[17] Recently, the other dimeric TtADPRase Ndx2 was suggested to follow a similar mechanism by the same research group.[18]

To examine the discrepancy between the mechanisms proposed for different ADPRases, we performed structure-based sequence alignment of the residues on the loop equivalent to loop L9 of hNUDT5. The residues of hNUDT5, MtADPRase,[15] EcADPRase[14], and TtADPRase Ndx2[18] are aligned based on their positions on the loop in the respective structures of these enzymes in complex with AMPCPR and metal ions representing the transition state (Fig. 2c). The analysis shows that Glu136 is the equivalent residue to Glu162 of EcADPRase and that the structure of the Ndx2–AMPCPR–Mg^{2+} complex is similar to that of the EcADPRase–AMPCPR–Mg^{2+} complex in that three metal ions are present at the active site and Glu136 also forms hydrogen-bonding interactions with the conserved water molecule. Moreover, mutation of Glu136 to Gln leads to a 12-fold decrease of the enzymatic activity and, additionally, conformational changes of the loop occur during catalysis.[18] Thus, we propose that Ndx2 also shares a similar catalytic mechanism with EcADPRase. As a corresponding structure of TtADPRase Ndx4 in complex with AMPCPR and metal ions is not available, sequence alignment was performed to predict the positions of the residues on the equivalent loop of Ndx4 (Fig. 2c). According to the sequence alignment, residues Asp126 and Glu129 of Ndx4 occupy similar positions as those of Glu162 of EcADPRase and Glu166 of hNUDT5, respectively (Fig. 2c). Intriguingly, mutation of either residue causes an 8-fold decrease in k_{cat}.[16] As the structure of the Ndx4–ADPR–Gd^{3+} complex was obtained under low pH and the enzyme is inactive under this condition (Ndx4 has 30% activity in the presence of Gd^{3+} relative to that in the presence of Mg^{2+}, but the substrate is not hydrolyzed in the complex[16]), the structure of Ndx4 in complex with AMPCPR and metal ions under more appropriate conditions needs to be determined to provide more precise information about the transition state, such as the number and positions of metal ions, and to understand the exact functional roles of Asp126 and Glu129 in catalysis. Nevertheless, due to the similarity between Ndx4 and Ndx2, it is very likely that Ndx4 might follow a similar mechanism as Ndx2. With all these data taken together, we propose that most dimeric eukaryotic and bacterial ADPRases utilize a similar mechanism of ADPR hydrolysis in which a conserved water molecule is rendered active by two coordinating metal ions and then attacks the α-phosphate of ADPR with the facilitation of an acidic residue on a loop at the active site, although there are variations in the movement of the loop during catalysis and in the position and the relative importance of the catalytic base.

Materials and Methods

Materials

ADPR was purchased from Sigma-Aldrich, and AMPCPR was synthesized as described by Pankiewicz *et al.*[26]

Cloning, expression, and purification of mutant hNUDT5

Site-directed mutagenesis was performed following the instruction for a QuikChange® Site-Directed Mutagenesis Kit (Strategene). The plasmid pGEX4T-1-ΔhNUDT5[20] containing a gene fragment corresponding to a truncated hNUDT5 (residues 1–210, ΔhNUDT5) was used as the template. The wild-type, truncated, and mutant hNUDT5 proteins were overexpressed and purified as described previously.[20]

Crystallization and diffraction data collection

The protein solution (20 mg/ml) was incubated with 5 mM AMPCPR and 10 mM $MgCl_2$ at 4 °C overnight before crystallization in hanging drops to obtain crystals of the enzyme in complex with AMPCPR. Crystals of ΔhNUDT5 in complex with AMPCPR and Mg^{2+} were grown at 4 °C from a drop consisting of equal volumes of the protein solution and the reservoir solution containing 250 mM NaAc, 100 mM Tris–HCl, pH 8.0, and 29% polyethylene glycol 4000. Single crystals of the plate-shape morphology grew after 1 month. Diffraction data were collected to 2.0-Å resolution from a flash-cooled crystal at beamline BL-6A of Photon Factory, Japan, and were processed using the *HKL*2000 suite.[27] The statistics of the diffraction data are summarized in Table 1.

Structure determination and refinement

The structure of ΔhNUDT5 in complex with AMPCPR and Mg^{2+} was solved using the molecular replacement method as implemented in the program CNS,[28] with the structure of ΔhNUDT5 in complex with ADPR [Protein Data Bank (PDB) code 2DSC] as the search model. There was well-defined electron density for the bound AMPCPR and three metal ions at the active site. The crystallization

condition for this complex is the same as that for the hNUDT5–ADPR complex except that ethylenediaminetetraacetic acid (EDTA) was present for the ADPR-bound complex while 10 mM $MgCl_2$ was supplemented for the AMPCPR-bound complex. Comparison of the structures of the hNUDT5–AMPCPR complex and the hNUDT5–ADPR complex shows that in the presence of EDTA, only one metal ion is present at the active site, while in the absence of EDTA and with the addition of $MgCl_2$, one metal ion is present at a similar position and two additional metal ions are bound at the active site. In addition, the position and coordination of the bound metal ions are analogous to the Mg^{2+} ions in the structure of the EcADPRase–AMPCPR–Mg^{2+} complex.[14] Therefore, we assigned these metal ions as Mg^{2+} ions. Structure refinement was performed with CNS using standard protocols (energy minimization, simulated annealing, and *B*-factor refinement), and model building was facilitated with program O.[29] The final structure refinement was carried out with the maximum-likelihood algorithm implemented in the program REFMAC5.[30] A bulk solvent correction and a free *R*-factor monitor (calculated with 5% of randomly chosen reflections) were applied throughout the refinement and model building. The stereochemical quality of the structure model was evaluated with the program PROCHECK.[31] A summary of the structure refinement statistics is given in Table 1.

Enzymatic activity assay

To measure the enzymatic activities of both wild-type and mutant hNUDT5 structures, we developed a new assay method by co-incubation of ADPR with the enzyme and alkaline phosphatase[16] coupled with a rapid and sensitive assay for quantitative analysis of the produced phosphate.[24] Specifically, 50 μl of reaction mixture was made of 50 mM Tris–HCl, pH 7.0, 5 mM $MgCl_2$, 1 mM DTT, 2 U of calf intestine alkaline phosphatase, 60–6000 nM concentration of the enzyme, and 0–10 mM ADPR. The reaction was performed at 37 °C for 10 min and then stopped by addition of 250 μl of 2.5% trichloroacetic acid. For measurement of the released P_i, 700 μl of phosphate determination reagent[24] (freshly prepared by mixing stock solutions of 1 ml of 0.2 M bismuth nitrate dissolved in 6 M nitric acid, 1 ml of 0.14 M ammonium molybdate, 0.5 ml of 1% ascorbic acid, and 2 ml of distilled water) was added, and the generated blue ternary heteropolyacid was quantitated at absorbance of 700 nm. The kinetic parameters were determined by fitting the initial rates of the reaction to the Michaelis–Menten equation. This new activity assay method is more rapid and sensitive than that by Yoshiba *et al.*,[16] and the kinetic parameters measured with the new method are comparable with those obtained with the previous method (Table 2). Biochemical data show that the enzymatic activity of the truncated ΔhNUDT5 is comparable with that of the full-length enzyme (Table 2). Thus, site-directed point mutations of important residues were introduced into ΔhNUDT5 for further kinetic studies.

PDB accession code

Coordinates and structure factors of the hNUDT5–AMPCPR–Mg^{2+} complex have been deposited in the Research Collaboratory for Structural Bioinformatics PDB with accession code 3BM4.

Acknowledgements

This work was supported by grants from the Ministry of Science and Technology of China (2004CB 720102, 2006AA02Z112, 2006AA02A313, and 2007C B914302), the National Natural Science Foundation of China (30570379, 30770480, and 30730028), the Chinese Academy of Sciences (KSCX2-YW-R-107), and the Science and Technology Commission of Shanghai Municipality (07XD14032 and 07ZR14131). We thank the staff members of Photon Factory, Japan, for their support in diffraction data collection.

References

1. Bessman, M. J., Frick, D. N. & O'Handley, S. F. (1996). The MutT proteins or "Nudix" hydrolases, a family of versatile, widely distributed, "housecleaning" enzymes. *J. Biol. Chem.* **271**, 25059–25062.
2. Gabelli, S. B., Bianchet, M. A., Bessman, M. J. & Amzel, L. M. (2001). The structure of ADP-ribose pyrophosphatase reveals the structural basis for the versatility of the Nudix family. *Nat. Struct. Biol.* **8**, 467–472.
3. Xu, W., Dunn, C. A., Jones, C. R., D'Souza, G. & Bessman, M. J. (2004). The 26 Nudix hydrolases of *Bacillus cereus*, a close relative of *Bacillus anthracis*. *J. Biol. Chem.* **279**, 24861–24865.
4. Olivera, B. M., Hughes, K. T., Cordray, P. & Roth, J. R. (1989). *Aspects of NAD metabolism in prokaryotes and eukaryotes*. ADP-ribose transfer reactions. Mechanisms and biological significance (Jacobson, M. K. & Jacobson, E. L., Eds.), Springer Verlag, New York, NY.
5. Haag, F. & Koch-Nolte, F. (1998). Endogenous relatives of ADP-ribosylating bacterial toxins in mice and men: potential regulators of immune cell function. *J. Biol. Regul. Homeostatic Agents*, **12**, 53–62.
6. Hassa, P. O., Haenni, S. S., Elser, M. & Hottiger, M. O. (2006). Nuclear ADP-ribosylation reactions in mammalian cells: where are we today and where are we going? *Microbiol. Mol. Biol. Rev.* **70**, 789–829.
7. Ueda, K. & Hayaishi, O. (1985). ADP-ribosylation. *Annu. Rev. Biochem.* **54**, 73–100.
8. McDonald, L. J. & Moss, J. (1994). Enzymatic and nonenzymatic ADP-ribosylation of cysteine. *Mol. Cell. Biochem.* **138**, 221–226.
9. Weigt, C., Just, I., Wegner, A. & Aktories, K. (1989). Nonmuscle actin ADP-ribosylated by botulinum C2 toxin caps actin filaments. *FEBS Lett.* **246**, 181–184.
10. Kwak, Y. G., Park, S. K., Kim, U. H., Han, M. K., Eun, J. S., Cho, K. P. *et al.* (1996). Intracellular ADP-ribose inhibits ATP-sensitive K^+ channels in rat ventricular myocytes. *Am. J. Physiol.* **271**, C464–C468.
11. Gasser, A., Glassmeier, G., Fliegert, R., Langhorst, M. F., Meinke, S., Hein, D. *et al.* (2006). Activation of T cell calcium influx by the second messenger ADP-ribose. *J. Biol. Chem.* **281**, 2489–2496.
12. Fliegert, R., Gasser, A. & Guse, A. H. (2007). Regulation of calcium signalling by adenine-based second messengers. *Biochem. Soc. Trans.* **35**, 109–114.
13. Mildvan, A. S., Xia, Z., Azurmendi, H. F., Saraswat, V., Legler, P. M., Massiah, M. A. *et al.* (2005). Structures and mechanisms of Nudix hydrolases. *Arch. Biochem. Biophys.* **433**, 129–143.
14. Gabelli, S. B., Bianchet, M. A., Ohnishi, Y., Ichikawa, Y., Bessman, M. J. & Amzel, L. M. (2002). Mechanism of the *Escherichia coli* ADP-ribose pyrophosphatase, a Nudix hydrolase. *Biochemistry*, **41**, 9279–9285.

15. Kang, L. W., Gabelli, S. B., Cunningham, J. E., O'Handley, S. F. & Amzel, L. M. (2003). Structure and mechanism of MT-ADPRase, a Nudix hydrolase from *Mycobacterium tuberculosis*. *Structure*, **11**, 1015–1023.
16. Yoshiba, S., Ooga, T., Nakagawa, N., Shibata, T., Inoue, Y., Yokoyama, S. *et al.* (2004). Structural insights into the *Thermus thermophilus* ADP-ribose pyrophosphatase mechanism via crystal structures with the bound substrate and metal. *J. Biol. Chem.* **279**, 37163–37174.
17. Ooga, T., Yoshiba, S., Nakagawa, N., Kuramitsu, S. & Masui, R. (2005). Molecular mechanism of the *Thermus thermophilus* ADP-ribose pyrophosphatase from mutational and kinetic studies. *Biochemistry*, **44**, 9320–9329.
18. Wakamatsu, T., Nakagawa, N., Kuramitsu, S. & Masui, R. (2008). Structural basis for different substrate specificities of two ADP-ribose pyrophosphatases from *Thermus thermophilus* HB8. *J. Bacteriol.* **190**, 1108–1117.
19. Shen, B. W., Perraud, A. L., Scharenberg, A. & Stoddard, B. L. (2003). The crystal structure and mutational analysis of human NUDT9. *J. Mol. Biol.* **332**, 385–398.
20. Zha, M., Zhong, C., Peng, Y., Hu, H. & Ding, J. (2006). Crystal structures of human NUDT5 reveal insights into the structural basis of the substrate specificity. *J. Mol. Biol.* **364**, 1021–1033.
21. Lin, S., Gasmi, L., Xie, Y., Ying, K., Gu, S., Wang, Z. *et al.* (2002). Cloning, expression and characterisation of a human Nudix hydrolase specific for adenosine 5′-diphosphoribose (ADP-ribose). *Biochim. Biophys. Acta*, **1594**, 127–135.
22. Yang, H., Slupska, M. M., Wei, Y. F., Tai, J. H., Luther, W. M., Xia, Y. R. *et al.* (2000). Cloning and characterization of a new member of the Nudix hydrolases from human and mouse. *J. Biol. Chem.* **275**, 8844–8853.
23. Gasmi, L., Cartwright, J. L. & McLennan, A. G. (1999). Cloning, expression and characterization of YSA1H, a human adenosine 5′-diphosphosugar pyrophosphatase possessing a MutT motif. *Biochem. J.* **344**, 331–337.
24. Chen, B., Guo, Q., Guo, Z. & Wang, X. (2003). An improved activity assay method for arginine kinase based on a ternary heteropolyacid system. *Tsinghua Sci. and Technol.* **8**, 422–427.
25. Dunn, C. A., O'Handley, S. F., Frick, D. N. & Bessman, M. J. (1999). Studies on the ADP-ribose pyrophosphatase subfamily of the Nudix hydrolases and tentative identification of trgB, a gene associated with tellurite resistance. *J. Biol. Chem.* **274**, 32318–32324.
26. Pankiewicz, K., Lesiak, K. & Watanabe, K. (1997). Efficient synthesis of methylenebis(phosphonate) analogues of P1,P2-disubstituted pyrophosphates of biological interest. A novel plausible mechanism. *J. Am. Chem. Soc.* **119**, 3691–3695.
27. Otwinowski, Z. & Minor, W. (1997). Processing of X-ray diffraction data collected in oscillation mode. *Methods Enzymol.* **276**, 307–326.
28. Brunger, A. T., Adams, P. D., Clore, G. M., DeLano, W. L., Gros, P., Grosse-Kunstleve, R. W. *et al.* (1998). Crystallography & NMR System: a new software suite for macromolecular structure determination. *Acta Crystallogr., Sect. D: Biol. Crystallogr.* **54**, 905–921.
29. Jones, T. A., Zou, J. Y., Cowan, S. W. & Kjeldgaard, M. (1991). Improved methods for building protein models in electron density maps and the location of errors in these models. *Acta Crystallogr., Sect. A: Found. Crystallogr.* **47**, 110–119.
30. Murshudov, G. N., Vagin, A. A. & Dodson, E. J. (1997). Refinement of macromolecular structures by the maximum-likelihood method. *Acta Crystallogr., Sect. D: Biol. Crystallogr.* **53**, 240–255.
31. Laskowski, R. A., MacArthur, M. W., Moss, D. S. & Thornton, J. M. (1993). PROCHECK: a program to check the stereochemical quality of protein structures. *J. Appl. Crystallogr.* **26**, 283–291.